

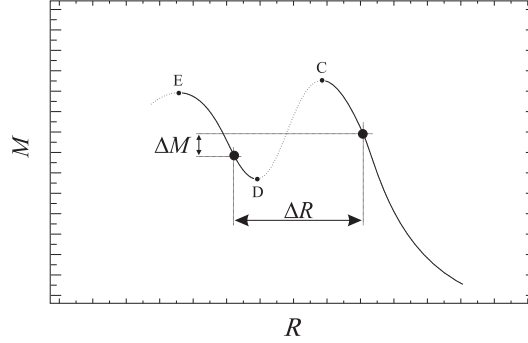
Quark phases in neutron stars and a “third family” of compact stars as a signature for phase transitions^{*}

K. Schertler^a, C. Greiner^a, J. Schaffner-Bielich^b, and M.H. Thoma^{c,†}

^a*Institut für Theoretische Physik, Universität Giessen
35392 Giessen, Germany*

^b*RIKEN BNL Research Center, Brookhaven National Laboratory
Upton, New York 11973-5000, USA*

^c*Theory Division CERN, CH-1211 Geneva 23, Switzerland*



Abstract

The appearance of quark phases in the dense interior of neutron stars provides one possibility to soften the equation of state (EOS) of neutron star matter at high densities. This softening leads to more compact equilibrium configurations of neutron stars compared to pure hadronic stars of the same mass. We investigate the question to which amount

^{*}Supported by DFG and GSI Darmstadt.

[†]Heisenberg Fellow.

the compactness of a neutron star can be attributed to the presence of a quark phase. For this purpose we employ several hadronic EOS in the framework of the relativistic mean-field (RMF) model and an extended MIT bag model to describe the quark phase. We find that - almost independent of the model parameters - the radius of a pure hadronic neutron star gets typically reduced by 20 – 30% if a pure quark phase in the center of the star does exist. For some EOS we furthermore find the possibility of a *third family* of compact stars which may exist besides the two known families of white dwarfs and neutron stars. We show how an experimental proof of the existence of a third family by mass and radius measurements may provide a unique signature for a phase transition inside neutron stars.

PACS: 12.38.Mh, 26.60.+c

Keywords: Quark matter; Neutron stars; Third family

1 Introduction

The properties of nuclear matter under extreme conditions are subject to intense experimental and theoretical studies in heavy-ion physics as well as in nuclear astrophysics. Especially neutron stars provide a unique astrophysical environment to study the properties of matter in the region of low temperatures and high baryonic densities. The densities deep inside neutron stars might be sufficient to populate numerous new forms of matter which may compete with each other. It is expected that at about two times normal nuclear matter density hyperons appear in neutron star matter [1, 2, 3, 4]. Also the formation of Bose-Einstein condensates [5, 6, 7] or the phase transition to deconfined quark matter have been considered [1, 2, 8, 9, 10, 11, 12]. For a recent review on possible phase transitions in neutron stars see [13]. However, our understanding of the properties of neutron star matter is still restricted due to theoretical limits and uncertainties in modeling the equation of state (EOS). Measurements of neutron star masses and radii may put important constraints on the EOS at large density. The masses of about twenty neutron stars (mainly pulsars in binary systems) have been measured and found to be quite near the “canonical” mass of $M = 1.4 M_{\odot}$ (M_{\odot} is the solar mass) [14]. Unfortunately, the currently known masses do not constrain the EOS unambiguously. While some soft EOS – which can only account for smaller masses – can be ruled out, it is not possible to differentiate between the class of stiffer EOS which give higher neutron star masses. However, these EOS can be classified by their different predictions for neutron star radii. Precise

measurements of neutron star radii can therefore give important information on the property of matter and possible exotic phases at large density. Some indirect radius estimates from observations of neutron stars seem to indicate surprisingly small radii. Recent radius estimates for Geminga (PSR 0630+17) by Golden and Shearer [15] suggest an upper bound of the apparent radius of $R_\infty \leq 9.5_{-2.0}^{+3.5}$ km for an assumed blackbody source and $R_\infty \leq 10.0_{-2.1}^{+3.8}$ km with the presence of a magnetized H atmosphere. Walter and Matthews obtained $R_\infty \lesssim 14$ km for the recently discovered isolated neutron star RXJ1856.5-3745 [16]. Generally the apparent radius R_∞ at a distance $d \rightarrow \infty$ is related to the local stellar radius R by

$$R_\infty = R / \sqrt{1 - 2GM/Rc^2}. \quad (1)$$

If we assume a mass of $M = 1.4 M_\odot$ an apparent radius R_∞ of about 11–13 km would restrict the radius to the quite low values of $R \approx 7–10$ km. (Due to (1), radii below $R_\infty \approx 11$ km would imply masses below $1.4 M_\odot$.) A radius of $R \lesssim 10$ km for a typical neutron star mass is furthermore consistent with the findings by Haberl and Titarchuk [17] for the X-ray burster 4U 1820-30, with the findings by Pavlov and Zavlin [18] for the millisecond pulsar J0437-4715 and by Li et al. [19] for Her X-1. (In the context of Ref. [19] see also Ref. [20] and Refs. [21, 22].) If radius estimates of $R \lesssim 10$ km indeed should prove to be reliable in connection with typical neutron star masses, the careful interpretation of these results in terms of neutron star matter properties would be an intriguing challenge for nuclear astrophysics. Since the appearance of a deconfined quark matter phase inside neutron stars is one possible mechanism to soften the EOS (and therefore to reduce the radius of the star), we want systematically address the question to which amount the compactness of a neutron star can be attributed to the presence of a quark phase. Such investigations are necessary also in view of more “exotic” interpretations of small radii e.g. in terms of “strange stars” [19, 23, 24]. It is important to study whether such interpretations are a consequence of ruling out other mechanisms suitable to soften the EOS at high densities (e.g. by hyperons, kaon condensates or quark phases) or provide only one possible explanation of the observed neutron star properties. For this purpose we will apply various hadronic EOS in the relativistic mean-field model (including hyperons) and a wide range of model parameters of the quark phase which we will describe in an extended MIT bag model.

The EOS of the hadronic and the quark phase will be discussed in Sec. 2. In Sec. 3 we discuss the construction of a first-order phase transition from hadronic to quark matter and present the results for the EOS. In Sec. 4 we

apply the EOS to the calculation of the neutron star structure and discuss the influence of quark phases. In Sec. 5 we discuss the properties of a possible “third family” of compact stars. Such hypothetical family of compact stars might exist besides the two known families of white dwarfs and neutron stars [25, 26, 27]. In this work we show how future measurements of masses and radii of only two compact stars may prove the existence of a third family. Moreover, we argue that this would provide a novel signature for a phase transition inside neutron stars, revealing a particular behavior of the EOS in the almost unknown regime of supernuclear densities. Finally, we summarize our findings in Sec. 6.

2 Equations of state

We want to start with a discussion of the different models used to describe the equation of state of “neutron star matter” i.e. cold, charge neutral matter in beta equilibrium. Neutron star matter covers a wide range of densities. Starting from the density of iron ($\epsilon \approx 8 \text{ g/cm}^3$) which builds the surface of a neutron star, densities up to few times normal nuclear matter density ($\epsilon_0 = 140 \text{ MeV/fm}^3 \approx 2.5 \times 10^{14} \text{ g/cm}^3$) can be achieved in the center of the star. Unfortunately there is yet no single theory capable to meet the demands of the various degrees of freedom opened up in neutron star matter in different densities regimes. We are therefore forced to use different models at different density ranges.

2.1 Subnuclear densities

For subnuclear densities we use the Baym-Pethick-Sutherland EOS [28], which describes the crust of the neutron star. Up to densities of $\epsilon \lesssim 10^7 \text{ g/cm}^3$ matter is composed of a Coulomb lattice of $^{56}_{28}\text{Fe}$ nuclei. The pressure is dominated by degenerate electrons. At higher densities nuclei become more and more neutron rich and at $\epsilon_{drip} \approx 4 \times 10^{11} \text{ g/cm}^3$ the most weakly bound neutrons start to drip out of the nuclei. For a detailed discussion of the Baym-Pethick-Sutherland EOS see [29]. A review of the properties of neutron rich matter at subnuclear densities can be found in [30].

2.2 Nuclear densities

The Baym-Pethick-Sutherland EOS is matched at $\epsilon \approx 10^{14} \text{ g/cm}^3 \approx \epsilon_0$ to a hadronic EOS calculated in the framework of the relativistic mean-field (RMF)

model. At these densities nuclei begin to dissolve and nucleons become the relevant degrees of freedom in this phase. The RMF model is widely used for the description of dense nuclear matter [31, 32, 3], especially in neutron stars. For an introduction into the RMF model see e.g. [1]. We use three EOS calculated by Schaffner and Mishustin in the extended RMF model [3] (i.e. TM1, TM2, GL85) and one by Ghosh, Phatak and Sahu [33]. For the latter one we use GPS as an abbreviation. These models include hyperonic degrees of freedom which typically appear at $\epsilon \approx 2 - 3\epsilon_0$. Table 1 shows the nuclear matter properties and the particle composition of the four EOS. Even

Hadronic EOS	TM1	TM2	GL85	GPS
reference	[3]	[3]	[3]	[33]
ρ_0 [fm $^{-3}$]	0.145	0.132	0.145	0.150
B/A [MeV]	-16.3	-16.2	-15.95	-16.0
K [MeV]	281	344	285	300
m_N^*/m_n	0.634	0.571	0.770	0.830
a_{sym} [MeV]	36.9	35.8	36.8	32.5
composition	a	a	a	b
a) n, p, e^- , μ^- , Λ , Σ^- , Σ^0 , Σ^+ , Ξ^- , Ξ^0				
b) n, p, e^- , μ^- , Λ , Σ^-				

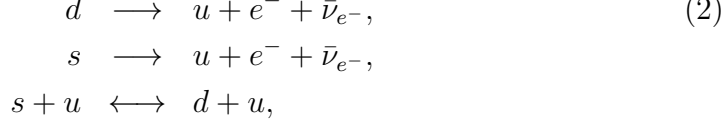
Table 1: Nuclear matter properties of the hadronic EOS. The saturation density and the binding energy is denoted by ρ_0 and B/A , the incompressibility by K , the effective mass by m_N^*/m_n and the symmetry energy by a_{sym} . The particle compositions are shown at the bottom of the table.

if the relevant degrees of freedom are specified (in our case basically nucleons and hyperons) the high density range of the EOS is still not well understood. The use of different hadronic models should reflect this uncertainty to some degree. In the following we will denote the phase described by the Baym-Pethick-Sutherland EOS and by the RMF model as the *hadronic phase* (HP) of the neutron star.

2.3 Quark matter

At densities above ϵ_0 we allow the HP to undergo a phase transition to a deconfined *quark matter phase* (QP). This section describes how we model the QP in weak equilibrium. The QP consists of u , d , s quarks and electrons in

weak equilibrium i.e. the weak reactions



imply relations between the four chemical potentials $\mu_u, \mu_d, \mu_s, \mu_e$ which read

$$\mu_s = \mu_d = \mu_u + \mu_e. \tag{3}$$

Since the neutrinos can diffuse out of the star their chemical potentials are taken to be zero. The number of chemical potentials necessary for the description of the QP in weak equilibrium (the number of components) is therefore reduced to two independent ones. We choose the pair (μ_n, μ_e) with the neutron chemical potential

$$\mu_n \equiv \mu_u + 2\mu_d.$$

In a pure QP (in contrast to a QP in a mixed phase, which we will discuss later) we have to require the QP to be charge neutral. This gives us an additional constraint on the chemical potentials

$$\rho_c^{QP} = \frac{2}{3}\rho_u - \frac{1}{3}\rho_d - \frac{1}{3}\rho_s - \rho_e = 0. \tag{4}$$

Here ρ_c^{QP} denotes the charge density of the QP and ρ_f ($f \in u, d, s$), ρ_e the particle densities of the quarks and the electrons, respectively. The EOS can now be parametrized by only one chemical potential, say μ_n . At this point it should be noted that the arguments given here for the QP also holds for the HP. There one also ends up with two independent chemical potentials (e.g. μ_n, μ_e) if one only requires weak equilibrium between the constituents of the HP, and with one chemical potential (e.g. μ_n) if one additionally requires charge neutrality. As we will discuss later, the number of independent chemical potentials plays a crucial role in the formulation of the Gibbs condition for chemical and mechanical equilibrium between the HP and the QP.

To calculate the EOS of the QP we apply the “effective mass bag model” [11, 34]. In this model, medium effects are taken into account in the framework of the MIT bag model [35, 36] by introducing density-dependent effective quark masses. The effective quark masses follow from the poles of the resummed one-loop quark propagator at finite chemical potential (see Fig. 1). Details of the calculation of the effective quark masses in the so called hard dense loop approximation can be found in [34]. One finds [34, 37]

$$m_f^*(\mu_f) = \frac{m_f}{2} + \sqrt{\frac{m_f^2}{4} + \frac{g^2\mu_f^2}{6\pi^2}}, \tag{5}$$

with the current quark mass m_f of the quark flavor f and the strong coupling constant g . These effective quark masses show the behavior of increasing mass with increasing density (chemical potential). For the current quark masses we choose $m_u = m_d = 0$ and $m_s = 150$ MeV. The effective masses (5) can now be used in the Fermi gas expression for the particle density

$$\rho_f(\mu_f) = \frac{d_f}{6\pi^2} [\mu_f^2 - m_f^{*2}(\mu_f)]^{3/2}, \quad (6)$$

where d_f is the degree of degeneracy [38]. The pressure p_f and energy density ϵ_f can be extracted from the thermodynamic relations

$$\rho_f(\mu_f) = \frac{dp_f(\mu_f)}{d\mu_f} \quad \text{and} \quad \epsilon_f(\mu_f) + p_f(\mu_f) = \mu_f \rho_f(\mu_f). \quad (7)$$

If $g \rightarrow 0$ the effective quark masses (5) approach the current quark mass m_f . In this limit, the EOS equals to a free MIT bag Fermi gas EOS. We therefore can use g to study the deviations from the free Fermi gas owing to the influence of medium effects. For this purpose we take g as a parameter ranging from $g = 0$ (no medium effects) to $g \approx 2 - 3$ ($\alpha_s \approx 0.31 - 0.72$). (It was found in [11] that a phase transition to a pure QP does not occur inside a typical neutron star for $g \gtrsim 2$. Larger values are therefore of minor interest for our purpose of studying the influence of quark phases on the properties of neutron stars.) The overall energy density ϵ_{QP} and pressure p_{QP} of the QP is the sum over all flavors plus the Fermi gas contribution ϵ_e, p_e of the uniform background of electrons plus the contribution of the phenomenological bag constant B .

$$\begin{aligned} \epsilon_{QP} &= \epsilon_u + \epsilon_d + \epsilon_s + \epsilon_e + B, \\ p_{QP} &= p_u + p_d + p_s + p_e - B, \end{aligned} \quad (8)$$

with

$$\epsilon_e = \frac{\mu_e^4}{4\pi^2} \quad \text{and} \quad p_e = \frac{\mu_e^4}{12\pi^2}. \quad (9)$$

The bag constant B is introduced in the usual way by adding it to the energy density and subtracting it from the pressure. Due to the phenomenological nature of the bag model, an exact value of B is not known. Therefore we will

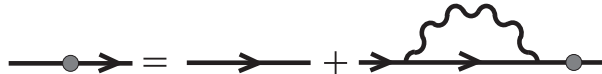


Figure 1: Resummed quark propagator.

take B as a free parameter ranging from $B^{1/4} = 165$ MeV ($B \approx 96$ MeV/fm³) to $B^{1/4} \approx 200$ MeV ($B \approx 208$ MeV/fm³). The lower bound of the bag constant is reasonable if one requires that the deconfinement phase transition to the QP should not occur at densities below $\epsilon \approx \epsilon_0$. We do not consider here the possibility of the existence of pure QP stars, so called “strange stars” or the related case of an absolutely stable QP (stable strange quark matter) with respect to the HP as it was supposed by Witten [39]. These possibilities are in detail discussed in the literature and we refer to [1, 2, 40, 41] for an overview. To find the QP to be absolutely stable, their energy per baryon E/A in equilibrium ($p_{QP} = 0$) must be lower than the energy per baryon of ⁵⁶Fe which is about 930 MeV. This requires small bag constants of $B^{1/4} \lesssim 155$ MeV (if we neglect medium effects). At our lower bound of the bag constant of $B^{1/4} = 165$ MeV we obtain an energy per baryon of $E/A \approx 990$ MeV which is about 60 MeV unbound with respect to ⁵⁶Fe. As one can imagine from (8), the bag constant plays a crucial role in the question whether or not a QP can exist in the interior of neutron stars.

3 Phase transition

Using the four EOS of the HP discussed in section 2.1 and 2.2 and the EOS of the QP discussed in the last section (2.3), we study the deconfinement phase transition from the HP to the QP and calculate the corresponding total EOS. In particular we are interested in the influence of the model parameters of the QP (i.e. the bag constant B and coupling constant g) on the phase transition densities. (The existence of a QP inside the neutron star clearly requires the transition density to be smaller than the central density of the star.) Before we come to this, we have first to discuss how to construct a first-order phase transition from the confined HP to the deconfined QP.

3.1 Construction of the phase transition

We calculate the phase transition according to Glendenning who has first realized the possibility of the occurrence of a mixed phase (MP) of hadronic and quark matter in a finite density range inside neutron stars [1, 42]. For simplicity we neglect Coulomb and surface effects in the MP as studied in Ref. [43]. The essential point in the calculation of the MP is that total charge neutrality can be achieved by a positively charged amount of hadronic matter and a negatively charged amount of quark matter. As already discussed in Sec. 2.3 we have to deal with two independent chemical potentials (μ_n, μ_e) if we impose

the condition of weak equilibrium. Such a system is called a *two-component system*. The Gibbs condition for mechanical and chemical equilibrium at zero temperature between the both phases reads

$$p_{HP}(\mu_n, \mu_e) = p_{QP}(\mu_n, \mu_e). \quad (10)$$

Using Eq. (10) we can calculate the equilibrium chemical potentials of the MP where $p_{HP} = p_{QP} \equiv p_{MP}$ holds. Fig. 2 illustrates this calculation for a specific choice of the model parameters (see figure caption). The HP→MP

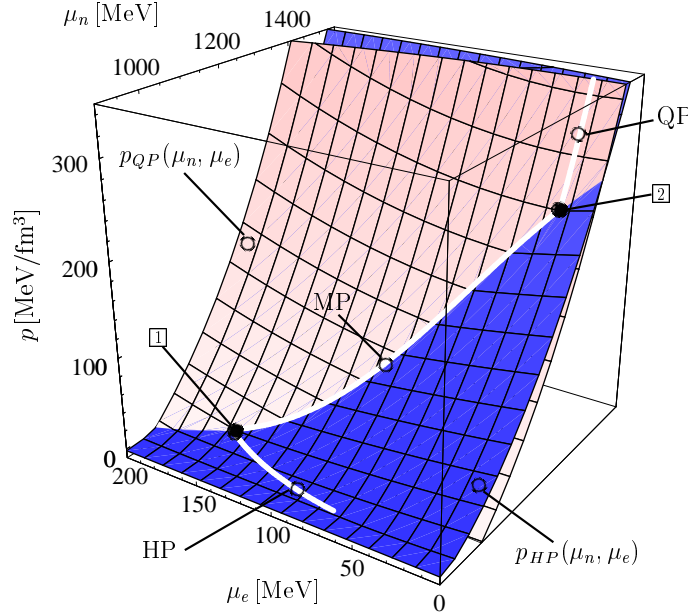


Figure 2: Gibbs phase construction of a two-component system. Plotted is the pressure of the hadronic phase p_{HP} and the pressure of the quark phase p_{QP} as a function of the two independent chemical potentials μ_n, μ_e . The white lines HP and QP on the pressure surfaces show the pressure of the hadronic phase and the quark phase under the condition of charge neutrality. At low pressure matter is in its charge neutral HP. At point 1 the HP reaches the intersection curve MP of the mixed phase. This curve is the solution of the Gibbs condition (10). At a pressure above point 2 matter consists of a pure QP. EOS of the HP is GPS, EOS of the QP uses $B^{1/4} = 170$ MeV and $g = 2$.

phase transition takes place if the pressure of the charge neutral HP (white line) meets the pressure surface of the QP. This happens at point 1 in Fig. 2. Up to this point the pressure of the QP is below the pressure of the HP,

making the HP the physically realized one. Up to point $\boxed{2}$ the phase follows the MP curve which is given by the Gibbs condition (10). At point $\boxed{2}$ the MP curve meets the charge neutral QP curve (white line) and the pressure of the QP is above the pressure of the HP, making the QP the physically realized one. The resulting chemical potentials are again shown in Fig. 3. Below the

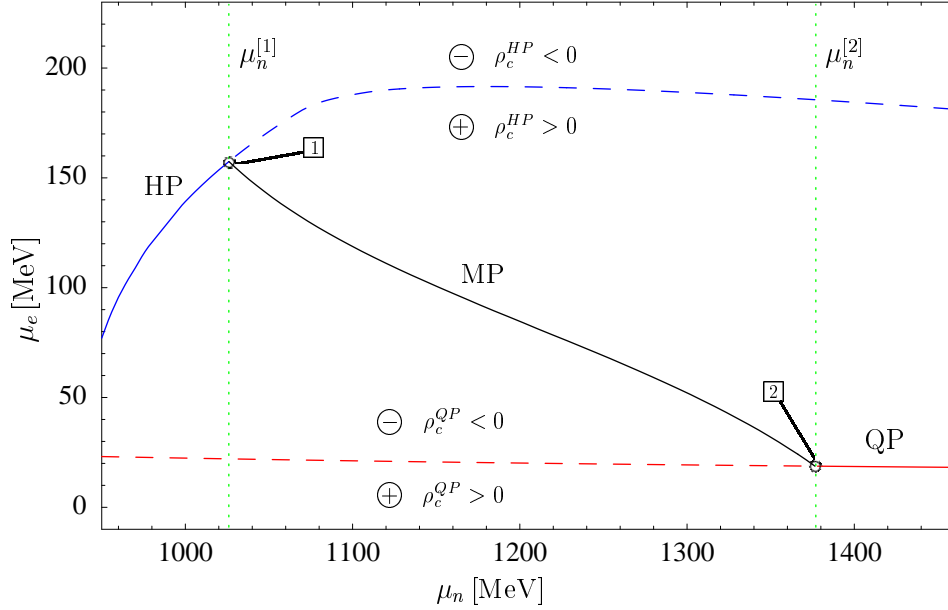


Figure 3: Electron chemical potential μ_e as a function of the neutron chemical potential μ_n . Up to $\mu_n^{[1]}$ matter is in its charge neutral HP. From $\mu_n^{[1]}$ to $\mu_n^{[2]}$ matter consists of a mixed phase (MP) of a charge positive HP ($\rho_c^{HP} > 0$, ρ_c denotes the charge density) and a charge negative QP ($\rho_c^{QP} < 0$). The MP curve is calculated from the Gibbs condition (10). Above $\mu_n^{[2]}$ matter consists of a pure charge neutral QP. EOS of the HP is GPS, EOS of the QP uses $B^{1/4} = 170$ MeV and $g = 2$.

charge neutral HP curve and above the charge neutral QP curve the HP is positively charged ($\rho_c^{HP} > 0$, ρ_c denotes the charge density) and the QP is negatively charged ($\rho_c^{QP} < 0$). Therefore, the charge of hadronic matter can be neutralized in the MP by an appropriate amount of quark matter. Up to the critical chemical potential $\mu_n^{[1]}$ the electron chemical potential of the charge neutral HP is increasing. (This is mainly because electrons have to neutralize the increasing amount of protons appearing in the HP.) At $\mu_n^{[1]}$ the phase transition to the MP takes place and μ_e can be reduced due to the first appearance of negatively charged quark phase droplets immersed in the

hadronic phase. (For a detailed discussion of the geometrical structure of the MP see [1].) For every point on the MP curve one has to calculate the volume proportion

$$\chi = \frac{V_{QP}}{V_{QP} + V_{HP}} \quad (11)$$

occupied by the quark phase by imposing the condition of global charge neutrality in the MP

$$\chi \rho_c^{QP} + (1 - \chi) \rho_c^{HP} = 0. \quad (12)$$

From this, the energy density ϵ_{MP} of the MP follows as

$$\epsilon_{MP} = \chi \epsilon_{QP} + (1 - \chi) \epsilon_{HP}. \quad (13)$$

In the MP the volume proportion of the quark phase is monotonically increasing from $\chi = 0$ at $\mu_n^{[1]}$ to $\chi = 1$ at $\mu_n^{[2]}$ where the transition into the pure QP takes place. Taking the charge neutral EOS of the HP (Sec. 2.2) for $\mu \leq \mu_n^{[1]}$, Eq. (10), (12) and (13) for the MP for $\mu_n^{[1]} < \mu_n < \mu_n^{[2]}$ and the charge neutral EOS of the QP (Sec. 2.3) for $\mu_n \geq \mu_n^{[2]}$ we can construct the full EOS in the form $p = p(\epsilon)$. For simplicity we denote the complete EOS as the *hybrid star* EOS.

As one realizes from Fig. 2, the phase transition construction in a two-component system leads to a monotonically increasing pressure of the MP with increasing density [42]. This is quite different from the constant pressure in a one-component system (with only one independent chemical potential) which neutron star matter is occasionally assumed to be. For the existence of a MP inside the star an increasing pressure is crucial. In turn, such a MP allows for a softer EOS over a wide density range which would be excluded in the one-component treatment. We will discuss this point in more detail in the appendix. There we show that a simplified treatment of the phase transition with only one independent component results in an overestimation of the phase transition density.

3.2 Results for the equation of state

In this section we present the results of the phase transition construction discussed in the last section. We study in particular the influence of different hadronic EOS and the influence of the model parameters of the QP on the properties of the phase transition. Fig. 4 shows the low density range of the hybrid star EOS in the form $p = p(\epsilon)$ for the four hadronic EOS and two coupling constants of the QP. The bag constant is chosen to be $B^{1/4} = 170$ MeV.

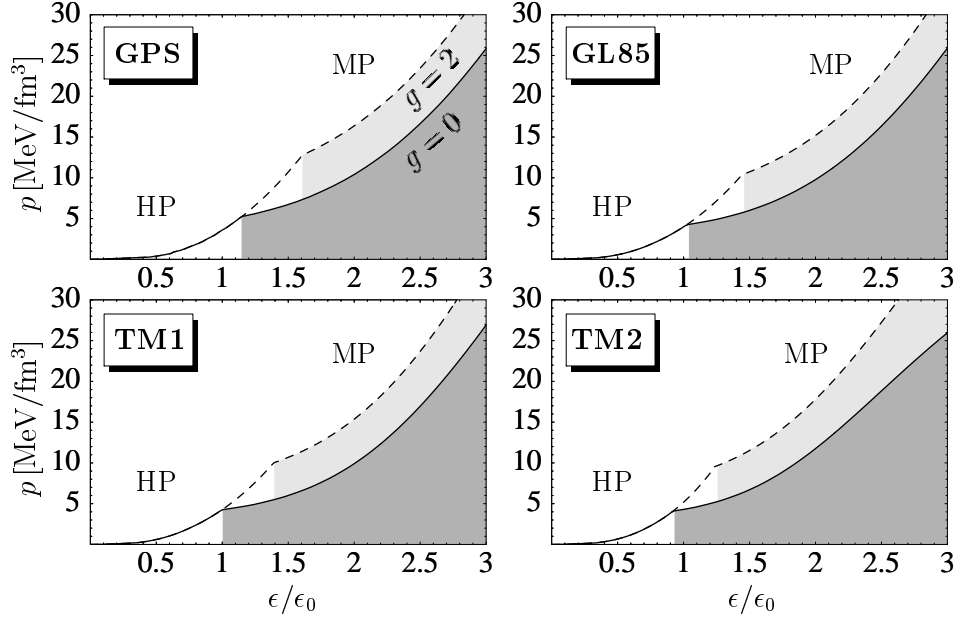


Figure 4: Low density range of the EOS for several hadronic EOS and two coupling constants g of the quark phase. The bag constant of the quark phase is chosen as $B^{1/4} = 170$ MeV. Shaded regions correspond to the mixed phase (MP) parts of the EOS. HP denotes the hadronic phase. $\epsilon_0 = 140 \text{ MeV/fm}^3$.

The MP part of the EOS is shaded gray. As already noted, even in the MP the pressure is monotonically increasing with increasing density. For that reason the MP does exist in the interior of the neutron star if its central energy density exceeds the HP→MP transition density. One can see that the HP→MP transition density depends only slightly on the choice of the hadronic EOS. This reflects the rather small uncertainty in the hadronic EOS in the density range up to about $1.5\epsilon_0$ where hyperonic degrees of freedom are still not present. (In the HP the hyperons typically appear at $2\text{--}3\epsilon_0$ [3].) The HP→MP transition density also depends only weakly on the influence of medium effects which shift the transition densities to slightly higher values. This was already found in [11]. Obviously the EOS gets softer compared to the HP due to the onset of the phase transition. (By “softer” we denote a smaller pressure at a fixed energy density ϵ .) In Fig. 5 we show the same hybrid star EOS in the high density region. In contrast to the HP→MP transition density we see that the MP→QP transition density is quite sensitive to the choice of the hadronic EOS as well as to the influence of medium effects in the QP. Assuming e.g. a star with a central energy density of $\epsilon = 5\epsilon_0$ we see that no

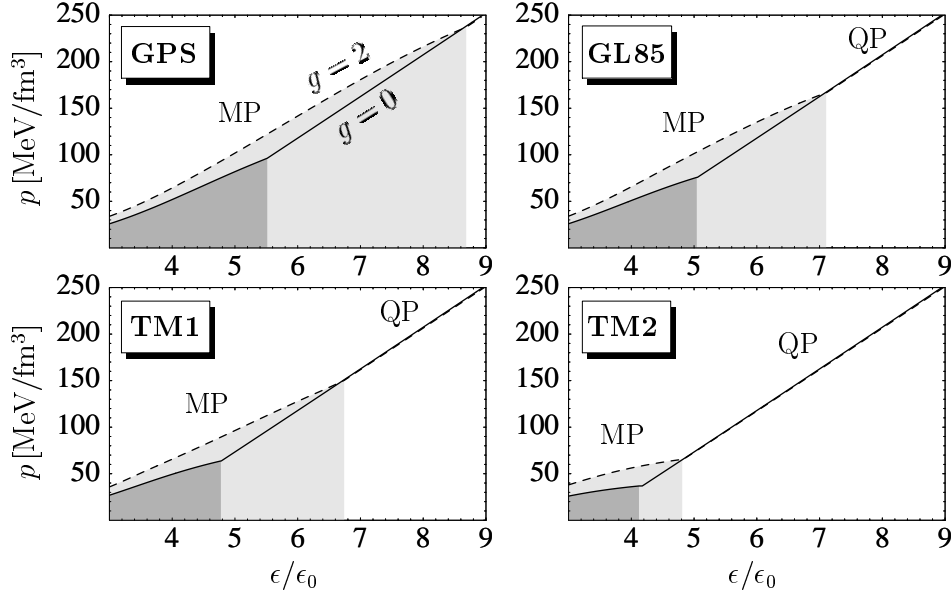


Figure 5: High density range of the hybrid star EOS of Fig. 4. The bag constant of the quark phase (QP) is chosen as $B^{1/4} = 170$ MeV. Shaded regions correspond to the mixed phase (MP) parts of the EOS. $\epsilon_0 = 140$ MeV/fm³.

conclusive statement can be made about the composition of the center of the star. Neglecting medium effects ($g = 0$), TM1 and TM2 predict a QP core (QC) while GPS and GL85 predict a MP core (MC). Taking medium effects into account ($g = 2$) only TM2 predicts a QC. The strong sensitivity of the transition densities can qualitatively be understood if we look again at Fig. 2. In the high pressure region where the MP→QP transition takes place, the HP and the QP pressure surfaces are nearly parallel. Therefore a small change in one EOS is able to produce considerably large changes in the MP→QP transition density. Furthermore one should note in Fig. 5 that (despite a change in the phase transition densities) the influence of medium effects on the pure QP EOS in the form $p = p(\epsilon)$ is negligible. This was already found in [34].

Up to now we have neglected the influence of the bag constant B which enters in the QP EOS. Since B enters negatively into the QP pressure in Eq. (8) a larger B will shift the pressure surface $p_{QP}(\mu_n, \mu_e)$ in Fig. 2 down which moves the MP intersection curve to higher pressures. This finally also shifts the transition densities to higher values. Fig. 6 and Fig. 7 demonstrate this behavior for different hybrid star EOS using GPS and TM2 for the HP (the other hybrid star EOS using TM1 and GL85 show a very similar behavior).

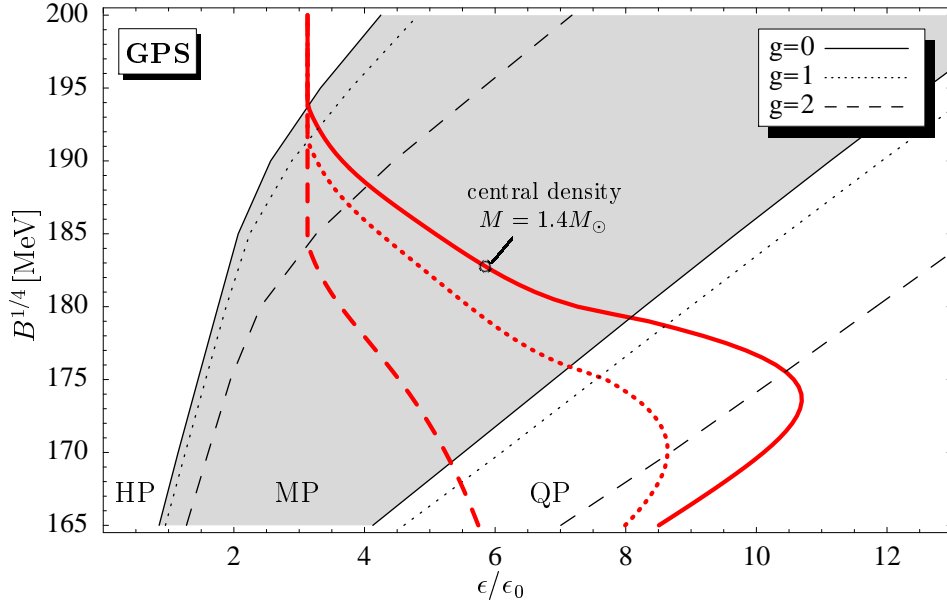


Figure 6: Phase transition densities for three different coupling constants g (thin lines) as a function of the bag constant B . The shaded region (MP) marks the density range of the MP at $g = 0$. The thick lines show the central energy density of a $1.4M_\odot$ star. As long as the thick line is to the right of the corresponding MP range (e.g. the shaded region for $g = 0$) the star possesses a pure quark phase core. $\epsilon_0 = 140 \text{ MeV/fm}^3$.

In these figures the gray shaded area corresponds to the density region of the MP for $g = 0$ (i.e. no medium effects). Obviously the HP \rightarrow MP and the MP \rightarrow QP transition densities are increasing with increasing B and increasing g where the MP \rightarrow QP transition density again is more sensitive. An increase of $B^{1/4}$ by only 5 MeV is able to increase the MP \rightarrow QP transition density by about one ϵ_0 . From Fig. 6 it is furthermore interesting to note that the HP \rightarrow MP transition density seems to be only slightly sensitive to a change of the model parameters as long as its density is below $\epsilon \approx 2\epsilon_0$ and strongly sensitive above (comparable to the MP \rightarrow QP transition density). This effect seems to be related to the appearance of hyperons (mainly Σ^- and Λ) in the HP EOS at densities of $\epsilon \approx 2-3\epsilon_0$ which has already been noted in [11].

It is important to note that the increase of the transition densities with increasing B does not necessarily disfavor the existence of deconfined phases inside the star since also the central energy density can be increased by changing this parameter. This is illustrated by the thick lines in Fig. 6 and Fig. 7

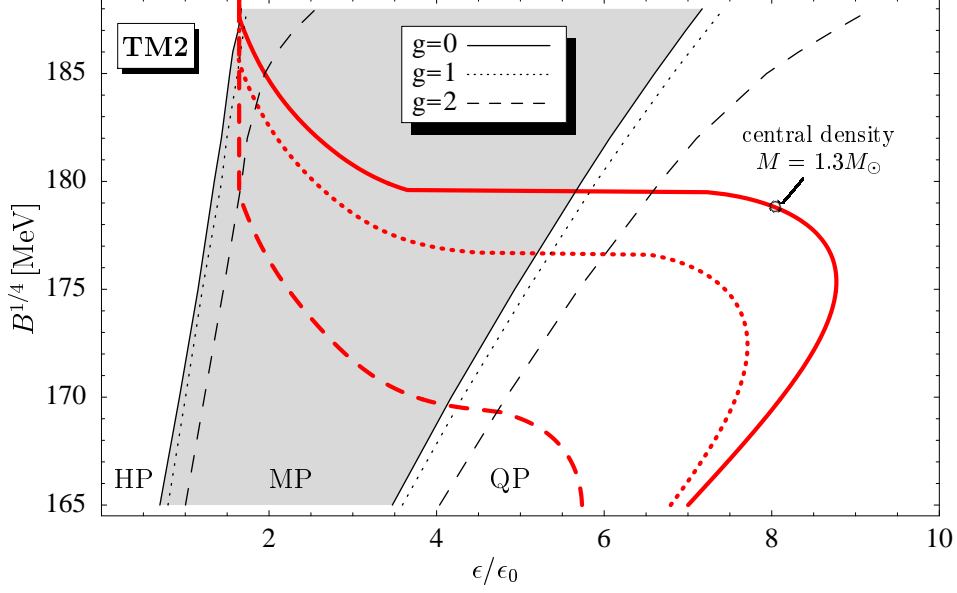


Figure 7: Phase transition densities for three different coupling constants g (thin lines) as a function of the bag constant B . The shaded region (MP) marks the density range of the MP at $g = 0$. The thick lines show the central energy density of a $1.3M_\odot$ star. $\epsilon_0 = 140 \text{ MeV/fm}^3$.

which show the central energy density of a star at fixed mass as a function of the bag constant. (The calculation of neutron star masses is discussed in the next section. In Fig. 7 we choose a mass of $M = 1.3 M_\odot$ instead of the “canonical” value of $M = 1.4 M_\odot$ since it turns out that for some (B, g) parameters the maximum mass (M_{max}) is slightly below $1.4 M_\odot$.) At least for $g = 0$ and $g = 1$ the central energy density is increasing with B for low values. From these figures we can already see which kind of phase (HP, MP or QP) is realized in the center of the star. E.g. from Fig. 6 we find that at $g = 0$ the central energy density (thick solid line) of a $M = 1.4 M_\odot$ star is above the MP→QP transition density for bag constants below $B^{1/4} \approx 180 \text{ MeV}$. In this parameter range the neutron star possesses a pure QP core (QC). At higher B up to $B^{1/4} \approx 195 \text{ MeV}$ the star possesses a MP core (MC). At still higher B the star is purely hadronic (HC). We will come back to a discussion of the (B, g) parameter range leading to one of the possibilities (QC, MC, HC) in the next section.

In the following we first want to focus in some more detail on the interesting behavior of the central energy density with increasing B . The central energy

density of a star at fixed mass depends on the softness or stiffness of the underlying EOS. Soft EOS possess a larger central energy density as compared to stiff EOS. In a simple way one could imagine that stars corresponding to soft EOS are compressed to smaller radii and therefore possess a larger central density. In our case (e.g. Fig. 6, thick line $g = 0$) two competing effects are important. By increasing B , i) the low density range of the hybrid star EOS gets stiffer due to an enlarged density range of the HP (which is stiffer than the MP) while ii) the density range of the QP gets softened directly by a larger bag constant. Effect ii) dominates for smaller B since large parts of the star are made of the QP. Therefore the central energy density is increasing with B . In both figures this holds up to about $B^{1/4} \approx 175$ MeV for $g = 0$. We will see in the next section that in this range the internal structure of the star is only slightly sensitive to a change of B because both the MP→QP transition density and the central energy density are equally increasing with B . The situation is reversed for bigger B and the central energy density is decreasing towards the value of the pure hadronic star. This behavior demonstrates two things. Firstly, the central energy density depends quite sensitively on the softness or stiffness of the EOS which effect the composition of neutron star matter. Thus it is not possible to talk about a “typical central energy density” of a neutron star without having a particular EOS in mind. Secondly, the increase of the bag constant – which makes the QP energetically less favorable – does not automatically disfavor the existence of a QP inside the star since also the central energy density is increased. Indeed, there is a region of the bag constant ($B^{1/4} \lesssim 175$ MeV) where the internal structure of the star depends only slightly on it. We will come back to this point below. We furthermore should note that the discontinuous fall of the central energy density in Fig. 7 for $g = 0$ at $B^{1/4} \approx 180$ MeV and for $g = 1$ at slightly lower B is related to the existence of “neutron star twins” which we will discuss in Sec. 5.

4 Neutron star structure

With the evaluated hybrid star EOS presented in the last section we now turn to analyse the structure of the corresponding non-rotating neutron stars by solving the Tolman-Oppenheimer-Volkoff (TOV) equations [44]. These equations describe the balance between the gravitational force and the pressure given by the Fermi pressure of the particular EOS. This leads to a relation between the mass M and the radius R of the neutron star in general relativistic hydrostatic equilibrium.

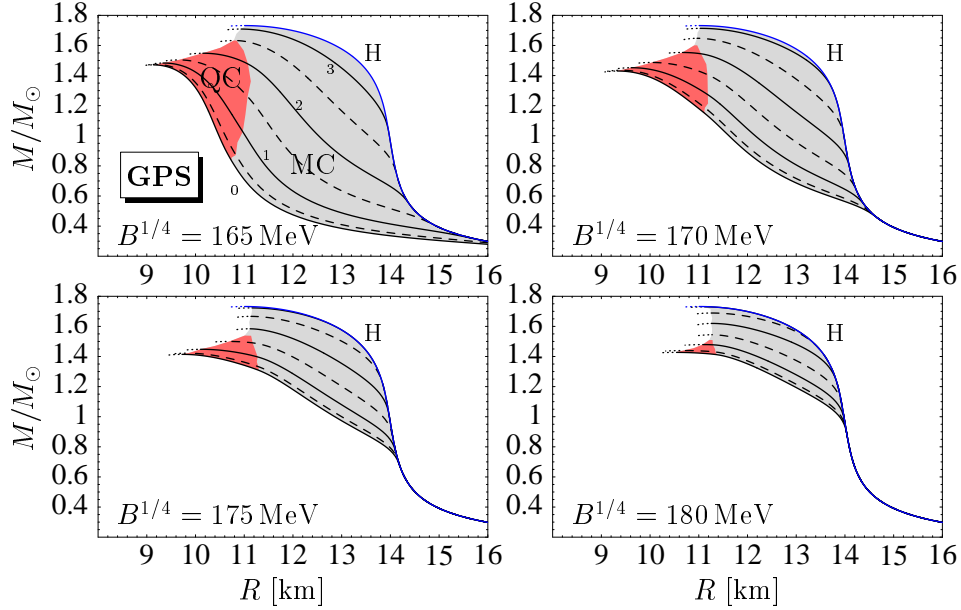


Figure 8: Mass-radius relations using the GPS EOS for the HP. The uppermost line denoted by H corresponds to the pure hadronic solution. All other curves allow for a phase transition to the quark phase. The small numbers denote the coupling constant g employed for the QP (dashed lines denote steps of 0.5 in g). Objects in the gray shaded MC region possess a mixed phase core while stars in the darker shaded QC region possess a pure quark phase core. Note the radius separation of about 2–4 km between the stars possessing a quark core and the pure hadronic stars of the same mass.

4.1 Mass-radius relations

Fig. 8 and Fig. 9 show the mass-radius (MR) relations for two hybrid star EOS (GPS and GL85) and several bag constants and coupling constants of the QP. The MR-relation denoted by H corresponds to the solution for the pure hadronic star (without any phase transition). The central energy density ϵ_c of the stars is increasing from large radii and small masses (down to the right) to the upper left edge where the *critical* central energy density ϵ_c^{crit} is reached at the maximum mass and the minimal radius of the star. From the two differently shaded regions denoted by QC (QP core) and MC (MP core) one sees whether ϵ_c is large enough to possess a QC or a MC in the center of the star. For small bag constants ($B^{1/4} \lesssim 180$ MeV) and small coupling constants (lower curves) ϵ_c is sufficient to exceed the MP \rightarrow QP transition density before

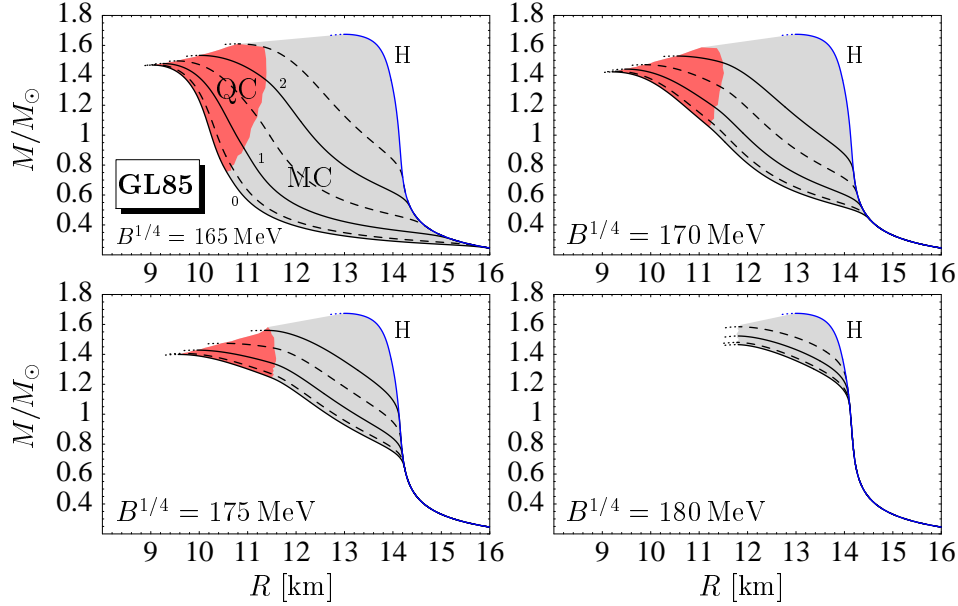


Figure 9: Mass-radius relations using the GL85 EOS for the HP. The upper-most line denoted by H corresponds to the pure hadronic solution. All other curves allow for a phase transition to the quark phase. The small numbers denote the coupling constant g employed for the QP (dashed lines denote steps of 0.5 in g). Stars in the gray shaded MC region possess a mixed phase core while stars in the darker shaded QC region possess a pure quark phase core.

ϵ_c^{crit} is reached (cf. Fig. 5). This leads to a pure QC inside the star. For a more detailed discussion of MR-relations and in particular of the influence of medium effects on the MR-relation see [11].

It is now our major aim to see what the effect of a pure QC on the mass and the radius of a neutron star is. Concerning the mass of the star we find that M_{\max} of a pure hadronic star (H) is reduced by about $0.1\text{--}0.3 M_{\odot}$ due to the phase transition and the corresponding softening of the EOS. Nevertheless, both hybrid star EOS are able to explain a typical neutron star mass of about $1.4 M_{\odot}$. The most compact objects seem to have radii of about $9\text{--}10$ km. In our model calculations these radii are only reached in stars possessing a pure QC (especially for $g \approx 0$). Very similar results are found for the two other hybrid star EOS (TM1 and TM2) which are not shown here. If we furthermore compare the radii of stars located in the QC region with the radii of the pure hadronic stars (H) of the same mass we can see that the QC stars are about $2\text{--}4$ km smaller than the corresponding hadronic stars. Hence, a neutron star

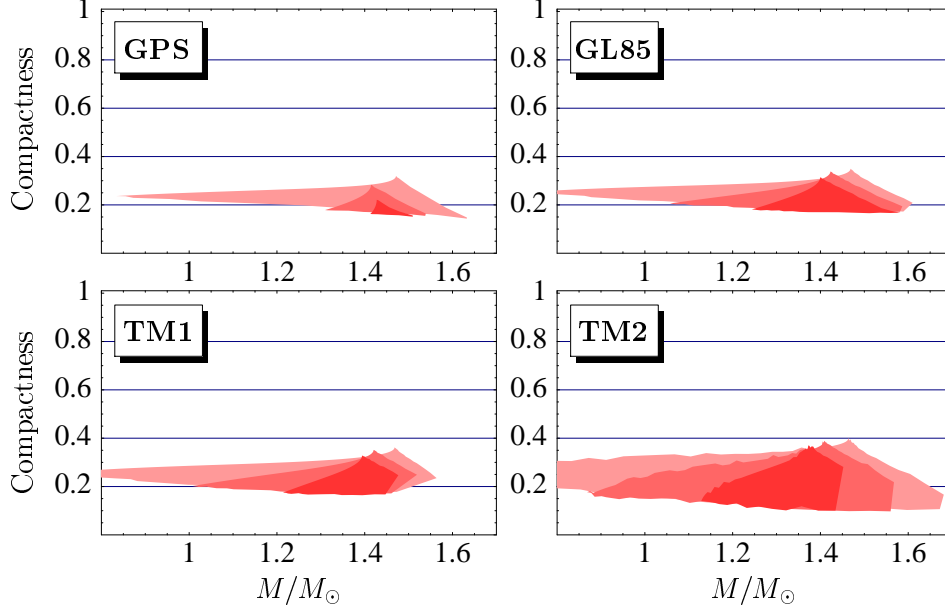


Figure 10: Compactness (14) of neutron stars possessing a pure quark core with respect to the pure hadronic star of the same mass. Obviously the presence of quark phases inside the star reduce the radius by typically 20–30%. The shaded areas stem from varying the model parameters of the quark phase (bag constant B (shading) and coupling constant g) which lead to a pure quark core inside the star. Especially for GPS, GL85 and TM1 the compactness ratio seems to be rather insensitive to the particular hadronic EOS and to the model parameters of the quark phase.

is about 20–30% more compact due to the presence of a pure QP in its center. We define the *compactness* of a neutron star possessing a QC as

$$\text{compactness}(M) \equiv \frac{R_H(M) - R_{QC}(M)}{R_H(M)}, \quad (14)$$

with the radius R_{QC} of the QC star and the radius R_H of the pure hadronic star of the same mass (cf. Figs. 8, 9). The compactness therefore corresponds to the ratio to which the radius of a pure hadronic star can be reduced due to the presence of a pure QP. The shaded areas in Fig. 10 come from calculating the compactness for all stars located in the QC region of the corresponding MR-relation (cf. Figs. 8, 9) for different bag constants (which are depicted in Fig. 10 by different shadings). It is remarkable that the compactness of 0.2–0.3 depend only slightly on the particular HP EOS and on the model

parameters applied in the QP. Especially an increase of the bag constant B (darker shading) only narrows the mass range leading to a QC. At the same time the range of the compactness is only slightly altered. A reduction of the radius of an hadronic star by 20–30% due to the presence of a pure QP seems to be a typical value. Only for $g \approx 0$ (which in general leads to the most compact stars) and the TM2 hybrid star EOS a radius reduction of about 40% seems possible (cf. Fig. 10). This might be related to a rather large incompressibility K , a small saturation density ρ_0 , and a small effective mass m_N^* of the TM2 EOS compared to the other EOS (cf. Tab. 1).

4.2 Internal structure

In this section we further study how the internal structure of the star e.g. the radius of the quark core (QC) or the thickness of the MP depends on the model parameters of the QP. Fig. 11 and Fig. 12 show the neutron star cross sections for a range of bag constants B and a *fixed* neutron star mass. The respective

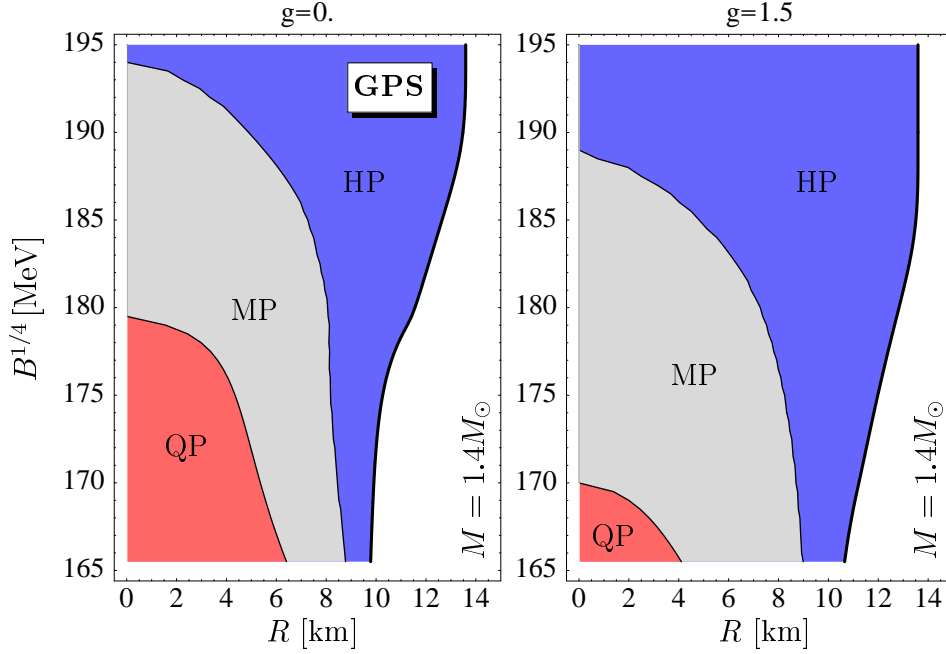


Figure 11: Internal structure of a $M = 1.4M_\odot$ neutron star as a function of the bag constant. Left panel $g = 0$ (no medium effects), right panel $g = 1.5$. The hadronic EOS is GPS.

left panels show the results without medium effects ($g = 0$) while the right

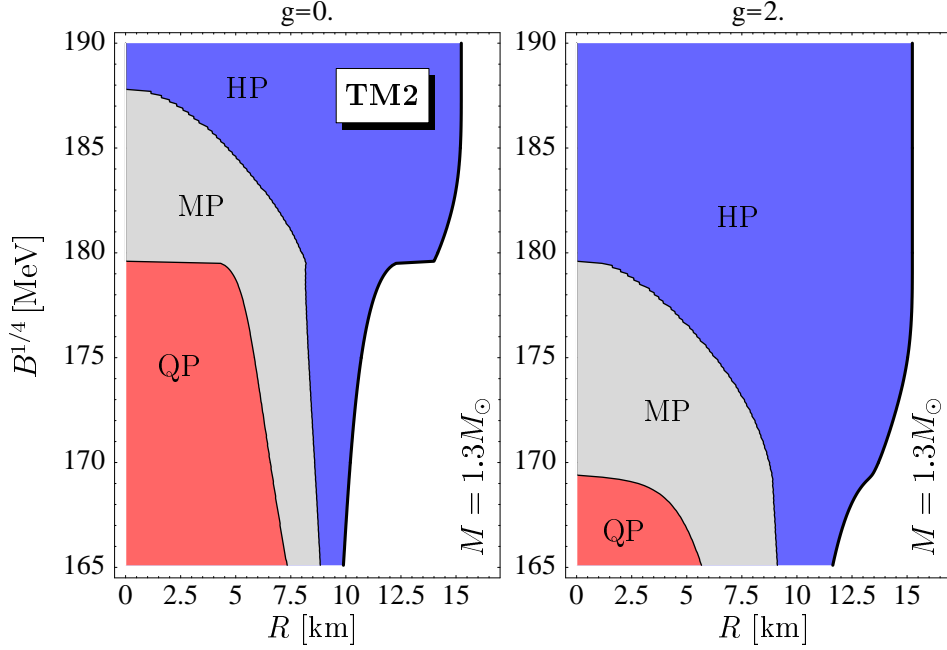


Figure 12: Internal structure of a $M = 1.3M_{\odot}$ neutron star as a function of the bag constant. Left panel $g = 0$ (no medium effects), right panel $g = 2$. The hadronic EOS is TM2.

panels include medium effects in the QP. The three differently shaded regions QP, MP and HP again correspond to the parts of the star made of quark phase, mixed phase and hadronic phase, respectively. The thick line to the right of the HP marks the surface of the star. It is obvious that basically only the presence of a pure QP is able to reduce the radius of the star significantly. For $g = 0$ (left panel) we can see in both figures that only for $B^{1/4} \lesssim 180$ MeV a pure QC can exist. For $B^{1/4} \lesssim 175$ MeV the radius of the QC can be as large as 4–7 km at an overall radius of about 10 km. For these values of B we can see that the internal structure of the star (especially the overall radius) only slightly depends on a change of B . This behavior can be traced back to the findings of Sec. 3.2. There we found that despite of an increase of B from $B^{1/4} = 165$ MeV to 175 MeV (which increases the MP→QP transition density in the GPS case by about $3\epsilon_0$) a pure QP is not excluded due to a similar increase of the central energy density ϵ_c (cf. Figs. 6 and 7).

On the right panels we can see how the influence of medium effects change the internal structure of the star. Since the HP→MP and MP→QP transition densities at fixed B increase with increasing g (cf. Fig. 6 and 7) medium effects

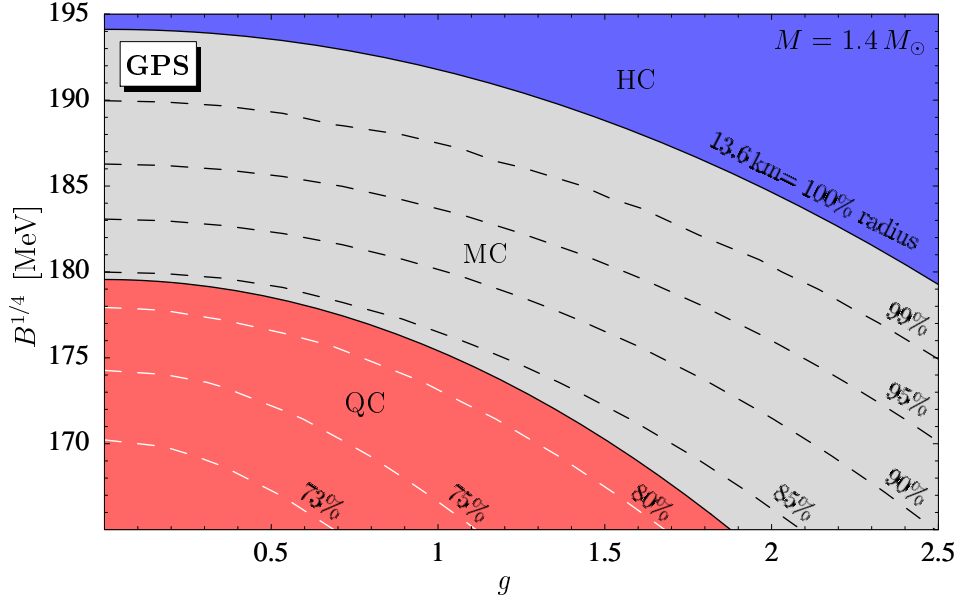


Figure 13: Parameter range (bag constant and coupling constant) of the internal structure of a $M = 1.4M_{\odot}$ neutron star. Parameters in the QC region lead to neutron stars with pure quark core while MC or HC corresponds to a mixed core or a pure hadronic star, respectively. The dashed lines are lines of constant radius given as the percentage of the radius of the hadronic star. The hadronic EOS is GPS.

are able to transform a star with MC into an pure hadronic star (e.g. Fig. 11, $B^{1/4} = 190$ MeV) or a star with QC to one with a MC (e.g. Fig. 11, $B^{1/4} = 175$ MeV). Only a lower bag constant can compensate for this effect to a certain degree. The solutions for the TM1 and GL85 hybrid star EOS (which are not shown here) lead to very similar results.

Finally, we illustrate the complete (B, g) parameter range in Fig. 13 and 14 to see which values lead to which kind of internal structure (QC, MC or HC (pure hadronic star)). Again we can see that - if we want to keep the internal structure of the star nearly fixed - the influence of medium effects can only be compensated by lowering the bag constant. The dashed lines show the neutron star radii in terms of the radius of the pure hadronic star. These lines correspond to lines of constant compactness (14). In both figures the borderline between the QC and the MC region appears at about 80% (corresponding to a compactness of 0.2). This demonstrates once more that - almost independently of the model parameters of the QP - a neutron star with a MC can at most be

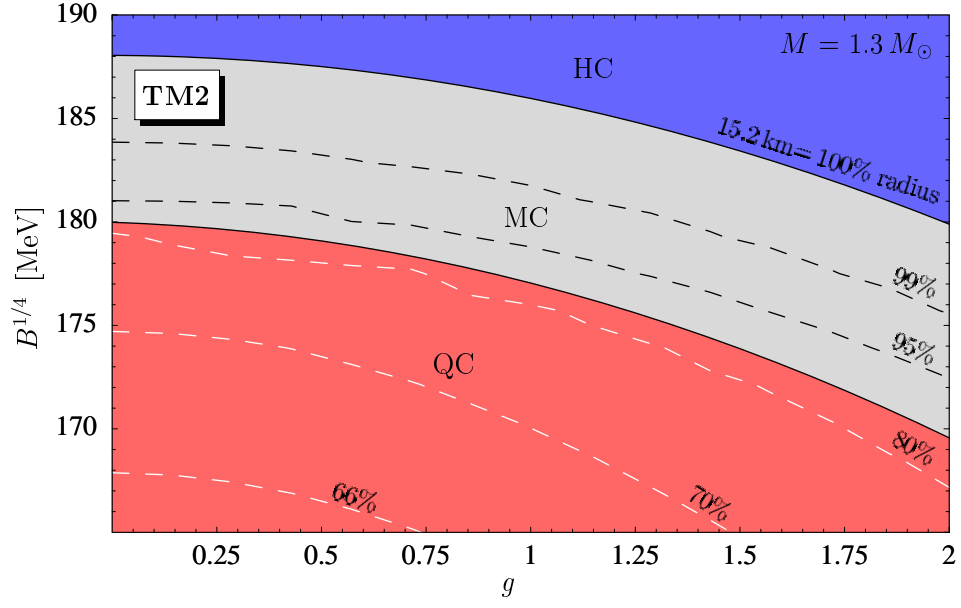


Figure 14: Same as Fig. 13 but for a neutron star mass of $M = 1.3M_{\odot}$. The hadronic EOS is TM2.

about 20% more compact than a hadronic star of the same mass while a star with a QC is typically 20–30% more compact than a hadronic star.

5 Phase transitions and the third family

5.1 Gerlach's criterion

Almost 30 years ago, it was found by Gerlach [25, 26] that a *third family* of stable equilibrium configurations of compact stars are not forbidden by general relativity. Such a third family could therefore in principle exist besides the two known families of white dwarfs and neutron stars. (See Fig. 15 for a schematic view of the three families in a MR-radius relation. The criteria for stability and instability of the shown ranges will be discussed in Sec. 5.3.). Gerlach

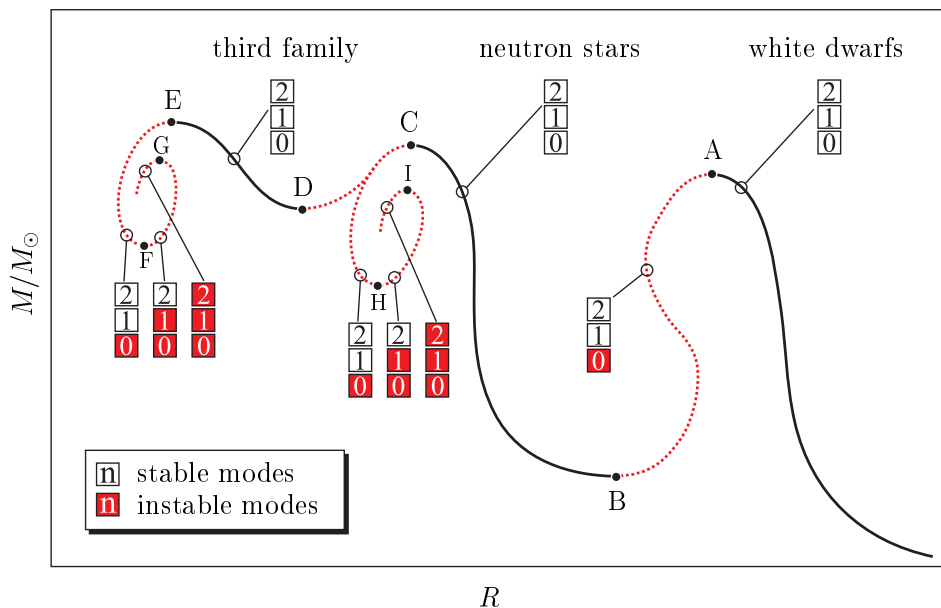


Figure 15: Schematic mass-radius relation showing three stable families of compact stars. The letters A, B, ..., I refer to critical points (turning points) where a vibrational mode changes stability [29, 45]. The stability (solid lines) or instability (dotted lines) of the three lowest-lying modes ($n = 0, 1, 2$) is depicted by the numbers. Higher modes are stable. See text for more details.

found that a *necessary* condition for the theoretical possibility of this family is a sufficiently large discontinuity in the speed of sound ($c_s^2 = dp/d\epsilon$) of the corresponding EOS¹. As the density is increased, the speed of sound has to increase abruptly at a density exceeding the central energy density of the

¹This was proved by means of an inversion of the Tolman-Oppenheimer-Volkoff equations. In this context see also the work by Lindblom [46].

neutron star of limiting mass (point C in Fig. 15). Rather smooth EOS (as comprehensively studied by Wheeler et al. [45]) does not possess the possibility of a third family. Thus a verification of the existence of a third family in nature is equivalent to the verification of a phase transition in the EOS of matter at large densities.

5.2 Quark phases and the third family

From Gerlach's criterion it remains however unclear i) which physical mechanism could produce a discontinuity (a phase transition) sufficient to support the stability of a third family and ii) whether a formation process exists in nature to physically realize these objects. Concerning i) it was recently found by Glendenning and Kettner [27] that certain EOS that describe a first-order phase transition to deconfined quark matter (like the EOS also considered in this work) could indeed lead to a third family. Due to partially overlapping mass regions of the neutron star branch and the branch of the third family it is possible that non-identical stars of the same mass can exist. Such pairs are referred to as “neutron star twins” [27]. In such kind of EOS the necessary discontinuity in the speed of sound is produced by the MP→QP transition of the deconfinement phase transition. As can be seen in our model from Fig. 5, especially the TM2 hybrid star EOS possesses a large discontinuity due to a rather low speed of sound at the high density end of the MP. In a particular parameter range of the bag constant we will see that the TM2 hybrid star EOS indeed allows for the existence of a third family². Fig. 16 shows MR-relations using the TM2 hybrid star EOS. They are shown for six different bag constants $B^{1/4}$ from 175 to 183 MeV. We furthermore assume $g = 0$ (no medium effects in the QP). The solutions for $B^{1/4} = 175$ MeV and $B^{1/4} = 183$ MeV do not lead to a third family and thus are similar to QC and MC solutions found in Figs. 8 and 9. Increasing the central density beyond the critical point does not restore stability (corresponding to range C-H-I in Fig. 15). This is not the case for bag constants in the small intermediate range $176 \text{ MeV} < B^{1/4} \leq 182 \text{ MeV}$. There the mass-radius relations are splitted by an instable (dotted) range which corresponds to C-D in Fig. 15. This enables the possibility of neutron star twins as shown e.g. for the low-density and high-density twin of mass $M = 1.36 M_\odot$. While the low-density twin (on the neutron star branch) has a MC the high-

²For the other hybrid star EOS we have checked more than 200 MR-relations following from different combinations of B and g without finding any further solutions including a third family. Since the parameter range for a third family seems to be quite small we might however have ignored some solutions.

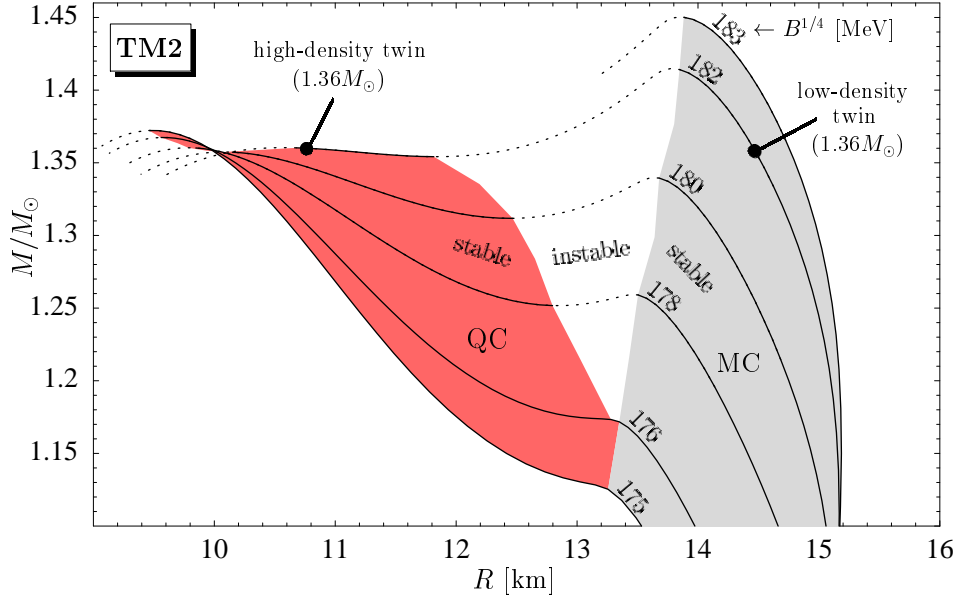


Figure 16: Mass-radius relation using the TM2 EOS for the HP for different bag constants B and $g = 0$. For this EOS a third family only exists in the narrow parameter range of $176 \text{ MeV} < B^{1/4} \leq 182 \text{ MeV}$. Obviously the stars of the third family possess approximately the same minimal radii as an “ordinary” hybrid star with pure QC as given by $B^{1/4} = 175 \text{ MeV}$.

density twin of the third family is more compact and possesses a QC. This is a general characteristic of neutron star twins [27]. The neutron star branch terminates in the MP owing to a small adiabatic index $\Gamma = (\epsilon + p)/p \cdot dp/d\epsilon$ (cf. Fig. 5) [27]. Thus, all stars on the neutron star branch are MC stars (or HC stars at lower ϵ_c). Only the larger adiabatic index of the QP can restore stability and therefore enables the QC stars of the third family. The internal structure of the neutron star twins with $M = 1.36 M_\odot$ is schematically shown in Fig. 17.

In this section we have seen, that from the deconfinement phase transition described in our model a sufficiently large discontinuity in the speed of sound arises to allow a third family of compact stars. This possibility was first realized by Glendenning and Kettner [27]. Despite the open questions concerning the existence of a formation process, we now want to ask for the theoretical possibility of identifying a third family by means of mass and radius measurements of neutron stars. To do so we have first to discuss the stability criteria which ultimately separate the third family branch of a MR-relation (range D-

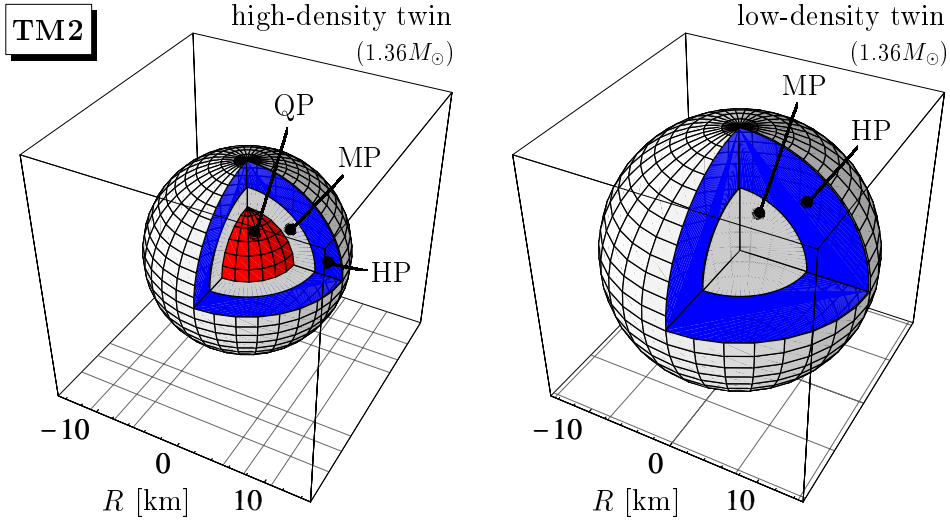


Figure 17: Schematic gross structure of the non identical neutron star twins marked in Fig. 16. Both stars have $M = 1.36M_\odot$ and belong to the same EOS (TM2 hybrid star EOS, $B^{1/4} = 182 \text{ MeV}$, $g = 0$).

E in Fig. 15) from the neutron star branch (range B-C) in the same way as neutron stars are separated from white dwarfs.

5.3 Stability criteria

While hydrostatic stability of stellar configurations is assured by means of the Tolman-Oppenheimer-Volkoff equations [44] a proof of dynamical stability requires an additional analysis of the radial vibration modes (acoustical modes) of the star. Due to dynamical instabilities no stable stars can have central densities in the range of about $10^9 - 10^{14} \text{ g/cm}^3$. This separates the family of the white dwarfs from the neutron star family. A configuration is stable against small perturbations around hydrostatic equilibrium if and only if the squared frequency eigenvalue ω_0^2 of the fundamental vibrational mode is positive [29, 45]. Dynamical stable and unstable parts of a schematic MR-relation are shown in Fig. 15. The letters A, B, ..., I refer to critical points (turning points) where $dM/d\epsilon_c = 0$ holds. The *central* energy density ϵ_c is rising from right to left along the curve A-C-I and A-C-G respectively. Reaching a critical point one radial vibrational mode (characterized by its number of nodes n) has to change stability. This means that the corresponding squared frequency eigenvalue ω_n^2 changes its sign [29, 45]. (A stable mode requires a positive squared frequency

$\omega_n^2 > 0$). At critical points where $dR/d\epsilon_c < 0$ holds (all points except H and F) an even mode changes stability while for $dR/d\epsilon_c > 0$ (points H and F) an odd mode changes stability [29, 45]. Starting from a stable neutron star located in the range B-C (all $\omega_n^2 > 0$) we reach the critical point C by increasing ϵ_c . At point C an even mode changes stability due to $dR/d\epsilon_c < 0$ and therefore gets instable. Since

$$\omega_0^2 < \omega_1^2 < \omega_2^2 < \dots < \omega_n^2 \quad (15)$$

holds [29, 45] this only can be the fundamental $n = 0$ mode. A perturbation would cause such instable star to explode or collapse to a black hole. The only way to recover stability and therefore to make a third family possible at larger density is a further change of stability of the even $n = 0$ mode at point D. (Note that point H can only change an odd mode). Due to (15) no even mode expect $n = 0$ can change stability at this critical point since all higher modes are bound by ω_1^2 which is still positive. For that reason the region D-E corresponding to the third family is again stable against radial vibrations. Without a sufficiently large discontinuity in the speed of sound (i.e. for any reasonably smooth EOS) the mass-radius relation follows the curve C-H-I [45, 47]. Increasing the central density then leads to a successive excitation of more and more unstable modes. (Only modes up to $n = 2$ are shown in Fig. 15).

As a important consequence of the stability analysis above, the mass and radius of point C has to be larger than the mass and radius of point D. Therefore it is possible that stars of the neutron star branch can in principle exist which are larger and heavier than stars of the third family.

5.4 The third family as a possible signature for a phase transition

Within our model we see from Fig. 16 that the masses and radii of the third family are comparable to the ones of the neighbouring $B^{1/4} = 175$ MeV MR-relation which does not possess a third family. Moreover, for a radius and mass of $R \approx 10$ km and $M \approx 1.35M_\odot$ we can see the interesting behavior that all branches of the third family intersect with the branch ($B^{1/4} = 175$ MeV) of the neutron star family in just one point. Only the existence of such an example (even though found in a particular model) illustrates that the measurement of the mass and the radius of only one star (even if exact) could in general not provide the information to decide whether this star is a neutron star or an object of the third family. But how much points on a MR-relation do we in principle have to know (to measure) to decide whether or not a third family

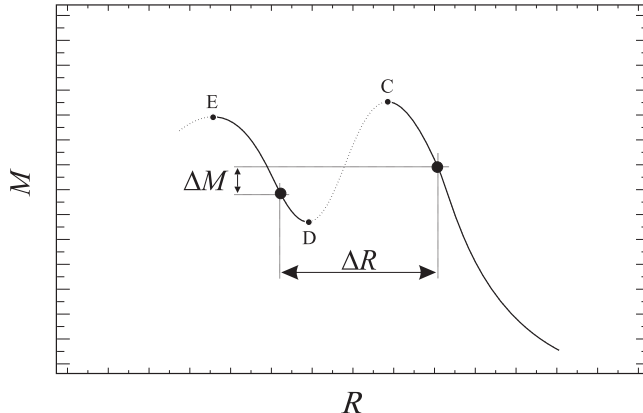


Figure 18: Schematic mass-radius relation showing a "rising twin" which can only exist if a third family of compact stars exists ($\Delta M \ll \Delta R$).

exists? The answer is *two*³. Comparing two arbitrary points on a neutron star MR-relation (e.g. $B^{1/4} = 175 \text{ MeV}$) we see that the heavier star always possesses the smaller radius. But this must not hold for MR-relations including a third family as discussed in the previous section. Then it is possible that the heavier star possesses the larger radius. Such pair of stars always exists if a third family exists. For that it is necessary that the smaller star is located on the third family branch while the larger star is on the neutron star branch. This is schematically shown in Fig. 18 where we have used the same notation as in Fig. 15. We will refer to such pair as a *rising twin*. The idea of a rising twin as a signature for a third family is therefore based on the decrease of the mass with increasing radius of all MR-relations without a third family. This holds for almost all *gravitational bound* stars in which an increase of mass leads to a decrease of the radius due to the increasing gravitational attraction (see also the Figs. 8, 9). An exception of this is given by *self-bound* stars like the hypothetical strange stars which show the behavior of increasing radius with increasing mass (for small masses $M \propto R^3$ holds) [1]. Also in some hadronic EOS (see e.g. [48]) mass ranges of slightly increasing radius with increasing mass can exist. However, we can exclude these exceptions by additionally require that $\Delta M \ll \Delta R$ ($G = c = 1$) has to hold for a rising twin. While in the case of a third family even $\Delta M = 0$ is allowed (the neutron star twin) this is not possible for the exceptions for which typically $\Delta M \gg \Delta R$ holds in

³For this it is important to note that the two masses and radii refer to two stars located on the *same* MR-relation. Therefore we can e.g. not refer to two stars with largely different temperature, magnetic field or rotational period.

the mass range of typical neutron stars. In the framework of our model (see Fig. 16) the corresponding radius differences can grow as large as $\Delta R \approx 3$ km at mass differences smaller than $\Delta M \approx 0.05 M_\odot \approx 0.07$ km ($M_\odot \approx 1.48$ km). For all possible rising twins of Fig. 16 ΔM is more than one order of magnitude smaller than ΔR . The requirement of small mass differences is furthermore not in contradiction to the experimentally known masses of neutron stars which are (at least for the classes of observed stars) in a remarkably narrow range of $M = 1.35 \pm 0.04 M_\odot$ [14]. In particular the mass differences of the two stars in some double neutron star binaries seems to be quite small⁴.

In applying the stability considerations of Sec. 5.3 we conclude that the detection of a rising twin (by the measurement of masses and radii of two neutron stars) can prove the existence of a third family of compact stars. Gerlach's criterion (Sec. 5.1) shows that this is equivalent to the existence of a phase transition in the EOS at finite density. The deconfinement phase transition (as discussed in this work) is one possible scenario that might explain the hypothetical third family of compact stars (Sec. 5.2).

6 Summary and conclusion

We have studied the properties of non-rotating cold neutron stars including the possibility of a phase transition to a deconfined quark phase (QP). To describe the confined hadronic phase (HP) of the star we have applied several hadronic EOS in the framework of the relativistic mean-field model (cf. Sec. 2.2, [3, 33]). The QP was modeled by an extended MIT bag model (effective mass bag model) which includes medium effects by means of effective medium dependent quark masses (cf. Sec. 2.3, [34, 11]). The influence of medium effects was parametrized by the strong coupling constant g . The construction of a first-order phase transition from confined to deconfined matter was performed by taking into account two independent chemical potentials (components) of neutron star matter (cf. Sec. 3, Fig. 2). This construction allows for the existence of a mixed phase (MP) of quark and hadronic matter over a finite range inside the star. We have systematically studied the influence of the model parameters of the QP (bag constant B , coupling constant g) on the EOS (see Figs. 4, 5), the phase transition densities (see Figs. 6, 7), the mass-radius rela-

⁴ For example the mass difference of the Hulse-Taylor pulsar PSR B1913+16 and its companion is $\Delta M \approx 0.05 M_\odot$ while the difference of PSR B1534+12 and its companion is even of the order of only $\Delta M \approx 10^{-3} M_\odot$ [14]. Of course the two stars of a rising twin must not necessarily build a binary system.

tions of the stars (see Figs. 8, 9) and the corresponding internal structure (see Figs. 11, 12). This analysis provides us with the information which parameters lead to neutron stars with pure quark phase core (QC), mixed phase core (MC) or with no phase transition at all (HC). We found that - almost independent of the model parameters of the quark phase and the applied hadronic EOS - the radius of neutron stars possessing a MC can at most be about 20% more compact than a pure hadronic star of the same mass. A neutron star possessing a MC would therefore - at least from its radius - be hardly distinguishable from a pure hadronic star. Stars with a QC, however, are typically 20–30% more compact than a hadronic star. This is depicted in Fig. 10 and Figs. 13, 14. The limitation to the upper value of 30% comes from our reasonable requirement that the deconfinement phase transition density should not appear below normal nuclear matter density. This approximately corresponds to $B^{1/4} \gtrsim 165 \text{ MeV}$ (c.f. Figs 6, 7). Within our model, the minimal radius of a neutron star is about 9–10 km at a corresponding mass of $1.4 - 1.5 M_{\odot}$. Such small radii of 9–10 km are only reached in neutron stars with a pure QC (as large as 4–7 km) and could not be explained using the pure hadronic models applied here. On the other hand, our models fail to explain radii of $R < 9 \text{ km}$. Although some radius estimates of neutron stars suggest quite small values [15, 16, 17, 18, 19, 21], the experimental limits (e.g. of distance measurements) and the uncertainties in the interpretation of the available data (e.g. by black-body fits) do currently not allow for a definite confirmation. Nevertheless, a future experimental confirmation of extreme small radii would offer a unique possibility to place new stringent constraints on the EOS at high densities. It is therefore necessary to study the theoretical limits of the compactness of neutron stars with inclusion of different softening mechanisms to disentangle the various scenarios in view of more restrictive future radius estimates.

In Sec. 5 we have discussed the theoretical possibility of a third family of compact stars which might exist besides the two known families of neutron stars and white dwarfs (c.f. Fig. 15). Within our model, we have shown that a deconfinement phase transition can explain the existence of such third family (c.f. Fig. 16). Compared to stars of the neutron star family, the stars of the third family can have similar masses while their radii can be up to about 3 km smaller. Without referring to our particular model for the EOS we argue that the availability of mass and radius measurements of only two compact stars can reveal the existence of a third family if the larger star is the (slightly) more massive one. We refer to such pair of stars as a *rising twin* (c.f. Fig. 18). By means of Gerlach's criterion (Sec. 5.1) the existence of a third family is equivalent to the existence of a phase transition in the EOS at large densities

(which not necessarily need to be the deconfinement phase transition). If reliable mass and radius measurements would be available, the detection of a rising twin could therefore serve as a novel signature for a phase transition inside neutron stars.

Acknowledgments: The authors thank S. Leupold for helpful discussions and for reading the manuscript. We thank P.K. Sahu for providing us with the GPS EOS. K.S. acknowledges the correspondence with U.H. Gerlach concerning the third family.

Appendix

In this appendix we intend to show that a simplified treatment of the phase transition construction like the one which appears in a one-component system (instead of a two-component system which neutron star matter in fact is) leads to an overestimation of the phase transition density. This is worth to point out since within a simplified treatment which occasionally is utilized for the construction of the phase transition one might exclude the possibility of quark phases inside neutron stars [42]. In a correct two component treatment, however, the onset of a mixed phase (MP) or a quark phase (QP) might already be occurred inside the star. Compared to the simplified treatment this results in more compact neutron star configurations due to a larger density range occupied by the soft MP or QP EOS.

The two-component system of neutron star matter in weak equilibrium can be reduced to a one-component one by requiring charge neutrality of the hadronic phase and the quark phase independently (i.e. locally) and not globally in the MP. As already discussed in Sec. 2.3, this reduces the number of independent chemical potentials (components) from two (e.g. μ_n, μ_e) to one (e.g. μ_n). (In the following one argument (μ_n) denotes charge neutral properties while two arguments (μ_n, μ_e) denotes charged ones.) The condition of local charge neutrality is of course unphysical in the sense that charge neutrality in the MP can also be achieved by means of the weaker (global) condition Eq. (12). Furthermore such a construction is thermodynamically incorrect if applied to neutron star matter. Whereas the Gibbs condition

$$p_{HP}(\mu_n) = p_{QP}(\mu_n), \quad (16)$$

of a one-component system does ensure the mechanical equilibrium and the chemical equilibrium of neutrons (and therefore of all uncharged particles) one

finds that the chemical equilibrium of the second component (μ_e) is in general not fulfilled in the MP i.e. (cf. Fig. 3)

$$\mu_e^{HP}(\mu_n) \neq \mu_e^{QP}(\mu_n). \quad (17)$$

Consequently, all charged particles of neutron star matter do not fulfill the condition of chemical equilibrium. The Gibbs condition (16) leads to the familiar first-order phase transition with a constant pressure MP. Since we know from the equations of hydrostatic equilibrium - the Tolman-Oppenheimer-Volkoff equations [44] - that the pressure has to increase if we go deeper into the star, a constant pressure MP is strictly excluded from the star. That is not the case for a two-component phase transition calculation, since the pressure is increasing with density even in the MP (see e.g. Fig. 2).

To show that the one-component treatment leads to an overestimation of the deconfinement phase transition density we go back to Fig. 3 where $\mu_n^{[1]}$ marks the critical chemical potential necessary for a HP→MP phase transition of the two-component system. All we have to show is that at $\mu_n^{[1]}$ the one-component system is still in its HP. In other words

$$p_{HP}(\mu_n^{[1]}) > p_{QP}(\mu_n^{[1]}) \quad (18)$$

must hold since at a fixed chemical potential the phase with the larger pressure is the physically realized one. The point \square in Fig. 2 and Fig. 3 is defined by the phase equilibrium between the charge neutral HP and the charged QP, which reads

$$p_{HP}(\mu_n^{[1]}) = p_{QP}(\mu_n^{[1]}, \mu_e^{[1]}). \quad (\text{point } \square \text{ in Fig. 2}) \quad (19)$$

Now we know that at fixed neutron chemical potential the charge density of the QP is given (in units of $|e|$) by

$$\rho_c^{QP}(\mu_n, \mu_e) = -\frac{\partial p_{QP}(\mu_n, \mu_e)}{\partial \mu_e}. \quad (20)$$

Since the QP is negatively charged at point \square (and everywhere above the charge neutral QP curve in Fig. 3) we find that the right hand side of (20) must also be negative. Therefore, at fixed μ_n (say $\mu_n^{[1]}$) the pressure is decreasing if we decrease μ_e from $\mu_e^{[1]}$ to the lower value at which the QP is charge neutral. This means

$$p_{QP}(\mu_n^{[1]}, \mu_e^{[1]}) > p_{QP}(\mu_n^{[1]}). \quad (21)$$

Putting (19) and (21) together, we finally obtain (18). This shows that due to the treatment of the phase transition as a simplified transition of a one-component system, the transition densities are shifted to higher values as compared to the ones expected from the correct treatment of neutron star matter as a two-component system.

References

- [1] N.K. Glendenning, *Compact Stars* (Springer-Verlag, 1997).
- [2] F. Weber, *Pulsars as Astrophysical Laboratories for Nuclear and Particle Physics* (IOP Publishing, 1998).
- [3] J. Schaffner and I.N. Mishustin, *Phys. Rev. C* 53 (1996) 1416.
- [4] S. Balberg and I. Lichtenstadt, G.B. Cook, *Astrophys. J. S.* 121 (1999) 515.
- [5] N.K. Glendenning, *Astrophys. J.* 293 (1985) 470.
- [6] N.K. Glendenning and J. Schaffner-Bielich, *Phys. Rev. Lett.* 81 (1998) 4564.
- [7] D.B. Kaplan and A.E. Nelson, *Phys. Lett. B* 175 (1986) 57;
 G.E. Brown, K. Kubodera, M. Rho, and V. Thorsson, *Phys. Lett. B* 291 (1992) 355;
 V. Thorsson, M. Prakash, and J.M. Lattimer, *Nucl. Phys. A* 572 (1994) 693;
 H. Fujii, T. Maruyama, T. Muto, and T. Tatsumi, *Nucl. Phys. A* 597 (1996) 645;
 G.Q. Li, C.-H. Lee, and G.E. Brown, *Phys. Rev. Lett.* 79 (1997) 5214.
- [8] G. Baym and S. Chin, *Phys. Lett. B* 62 (1976) 241.
- [9] G. Chapline and M. Nauenberg, *Nature* 264 (1976) 235;
 B.D. Keister and L.S. Kisslinger, *Phys. Lett. B* 64 (1976) 117;
 B. Freedman and L. McLerran, *Phys. Rev. D* 17 (1978) 1109.
- [10] *Strange Quark Matter in Physics and Astrophysics*, edited by J. Madsen and P. Haensel, *Nucl. Phys. B (Proc. Suppl.)* 24B.

- [11] K. Schertler, P.K. Sahu, C. Greiner, and M.H. Thoma, Nucl. Phys. A637 (1998) 451.
- [12] K. Schertler, S. Leupold, and J. Schaffner-Bielich, Phys. Rev. C60 (1999) 025801.
- [13] H. Heiselberg and M. Hjorth-Jensen, nucl-th/9902033, report commissioned for Physics Reports.
- [14] S.E. Thorsett, Z. Arzoumanian, M.M. McKinnon, and J.H. Taylor, Astrophys. J. 405 (1993) L29;
S.E. Thorsett and D. Chakrabarty, Astrophys. J. 512 (1999) 288.
- [15] A. Golden and A. Shearer, Astron. Astrophys. 342 (1999) L5.
- [16] F.M. Walter, S.J. Wolk, and R. Neuhauser, Nature 379 (1996) 233;
F.M. Walter and L.D. Matthews, Nature 389 (1997) 358.
- [17] F. Haberl and L. Titarchuk, Astron. Astrophys. 299 (1995) 414.
- [18] G.G. Pavlov and V.E. Zavlin, Astrophys. J. 490 (1997) L91.
- [19] X.-D. Li, Z.-G. Dai, and Z.-R. Wang, Astron. Astrophys. 303 (1995) L1.
- [20] I. Wasserman and S.L. Shapiro, Astrophys. J. 265 (1983) 1036.
- [21] A.P. Reynolds, P. Roche, and H. Quaintrell, Astron. Astrophys. 317 (1997) L25.
- [22] J. Madsen, Astron. Astrophys. 318 (1997) 466.
- [23] I. Bombaci, Phys. Rev. C55 (1997) 1587.
- [24] M. Dey, I. Bombaci, J. Dey, S. Ray, and B.C. Samanta, Phys. Lett. B438 (1998) 123.
- [25] U.H. Gerlach, Phys. Rev. 172 (1968) 1325.
- [26] U.H. Gerlach, Ph.D. thesis, A third family of stable equilibria, Princeton University, 1968 (unpublished).
- [27] N.K. Glendenning and C. Kettner, Astron. Astrophys. 353 (2000) L9.

- [28] G. Baym, C.J. Pethick, and P. Sutherland, *Astrophys. J.* 170 (1971) 299;
R.P. Feynman, N. Metropolis, and E. Teller, *Phys. Rev.* 75 (1949) 1561;
G. Baym, H.A. Bethe, and C.J. Pethick, *Nucl. Phys.* A175 (1971) 225.
- [29] S.L. Shapiro and S.A. Teukolsky, *Black Holes, White Dwarfs, and Neutron Stars*, (John Wiley & Sons, N.Y., 1983).
- [30] C.J. Pethick and D.G. Ravenhall, *Annu. Rev. Nucl. Part. Sci.* 45 (1995) 429.
- [31] N.K. Glendenning, F. Weber, and S.A. Moszkowski, *Nucl. Phys.* A572 (1994) 693;
J.I. Kapusta and K.A. Olive, *Phys. Rev. Lett.* 64 (1990) 13;
J. Ellis, J.I. Kapusta, and K.A. Olive, *Nucl. Phys.* B348 (1991) 345.
- [32] N.K. Glendenning, *Phys. Lett.* B114 (1982) 392;
N.K. Glendenning, *Z. Phys.* A327 (1987) 295.
- [33] S.K. Ghosh, S.C. Phatak, and P.K. Sahu, *Z. Phys.* A352 (1995) 457.
- [34] K. Schertler, C. Greiner, and M.H. Thoma, *Nucl. Phys.* A616 (1997) 659.
- [35] A. Chodos, R.L. Jaffe, K. Johnson, C.B. Thorn, and V.F. Weisskopf, *Phys. Rev.* D9 (1974) 3471;
A. Chodos, R.L. Jaffe, K. Johnson, and C.B. Thorn, *Phys. Rev.* D10 (1974) 2599.
- [36] E. Farhi and R.L. Jaffe, *Phys. Rev.* D30 (1984) 2379.
- [37] V.V. Klimov, *Sov. Phys. JETP* 55 (1982) 199;
H.A. Weldon, *Phys. Rev.* D26, (1982) 2789;
H. Vija and M.H. Thoma, *Phys. Lett.* B342 (1995) 212;
J.-P. Blaizot and J.-Y. Ollitrault, *Phys. Rev.* D48 (1993) 1390.
- [38] M.I. Gorenstein and S.H. Yang, *Phys. Rev.* D52 (1995) 5206.
- [39] A.R. Bodmer, *Phys. Rev.* D4 (1971) 1601;
E. Witten, *Phys. Rev.* D30 (1984) 272.
- [40] J. Madsen, astro-ph/9809032, to appear in 'Hadrons in Dense Matter and Hadrosynthesis', ed. J. Cleymans (Lecture Notes in Physics, Springer Verlag).

- [41] C. Greiner and J. Schaffner, Int. J. Mod. Phys. E5 (1996) 239;
C. Greiner and J. Schaffner-Bielich, nucl-th/9801062, to appear in 'Heavy Elements and Related New Phenomena', ed. R.K. Gupta and W. Greiner (World Scientific Publications).
- [42] N.K. Glendenning, Phys. Rev. D46 (1992) 1274.
- [43] H. Heiselberg, C.J. Pethick, and E.F. Staubo, Phys. Rev. Lett. 70 (1993) 1355.
- [44] J.R. Oppenheimer and G.M. Volkoff, Phys. Rev. 55 (1939) 347;
R.C. Tolman, Phys. Rev. 55 (1939) 364.
- [45] B.K. Harrison, K.S. Thorne, M. Wakano, and J.A. Wheeler, Gravitation Theory and Gravitational Collapse, University of Chicago Press, Chicago 1965.
- [46] L. Lindblom, Astrophys. J. 398 (1992) 569.
- [47] Ch. Kettner, F. Weber, M.K. Weigel, and N.K. Glendenning, Phys. Rev. D51 (1995) 1440.
- [48] A. Akmal, V.R. Pandharipande, D.G. Ravenhall, Phys. Rev. C58 (1998) 1804.